

Figure S2. Example phage tRNA-Seq tracts, related to STAR Methods. The tail is modified into CCA, even it is not encoded as CCA within the genome. Here, “ref” indicates the genomic tRNA sequence for phage 2.275.O. The best match *E. coli* or T4 phage tRNA sequences and modifications are shown for comparison (“coli”). Finally, the base distribution at each position was used to fit a model for how modifications correspond to “missequenced” reads (“model”). Colors indicate bases (C, green; G, purple; A, magenta; T, blue), and represent the original genomic base at a given alignment position. Black bars beneath indicate coverage at a particular base. A full summary of all tRNA modification calls is available on Genbank (BioProject number PRJNA524872).

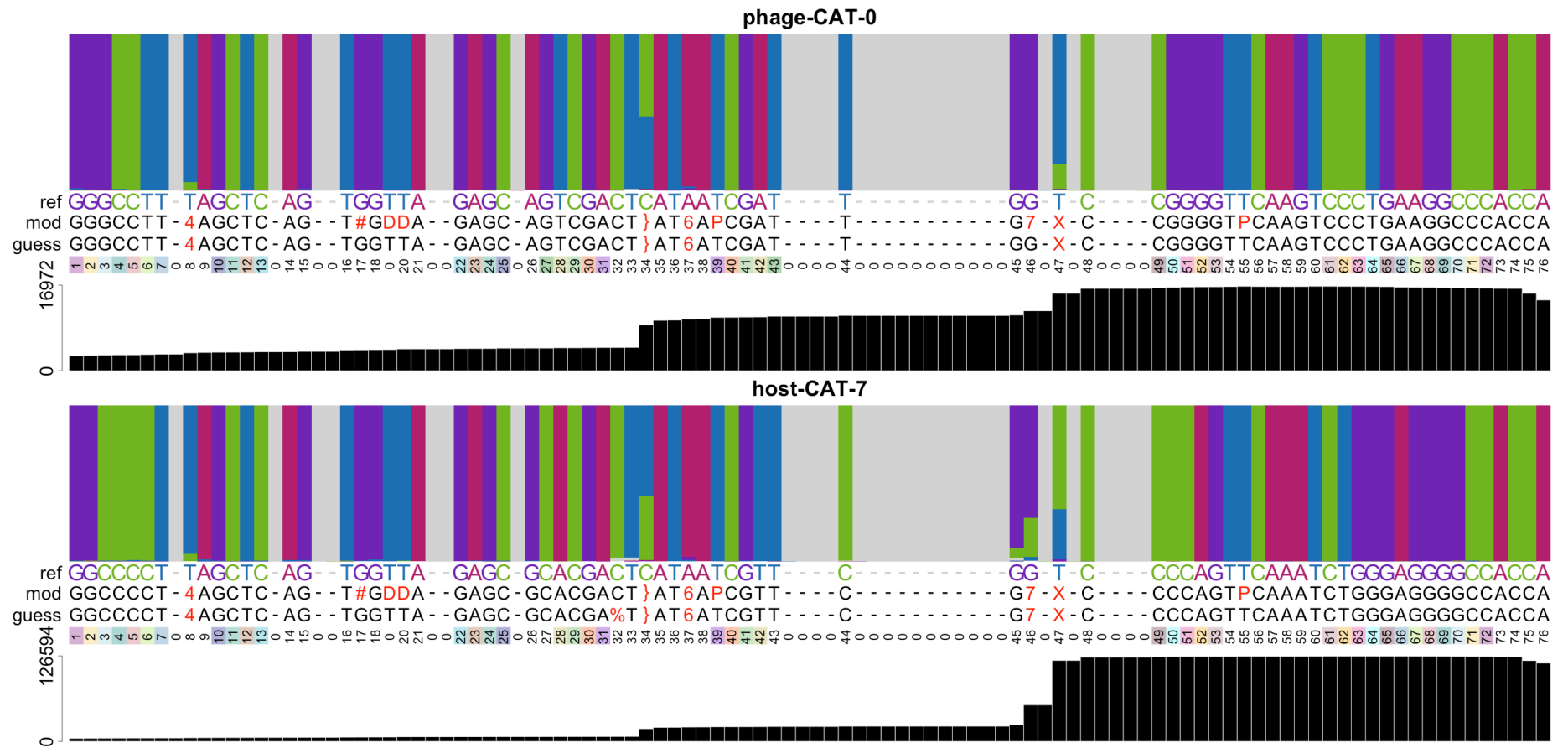


Figure S3. Example tRNA tracts comparing Ileu-}AT tRNA from the host (10N.286.54.E11), and from the phage (2.275.O), related to STAR Methods. Their genomic sequences are denoted as (“ref”). A full summary of all tRNA modification calls is available on Genbank (BioProject number PRJNA524872).

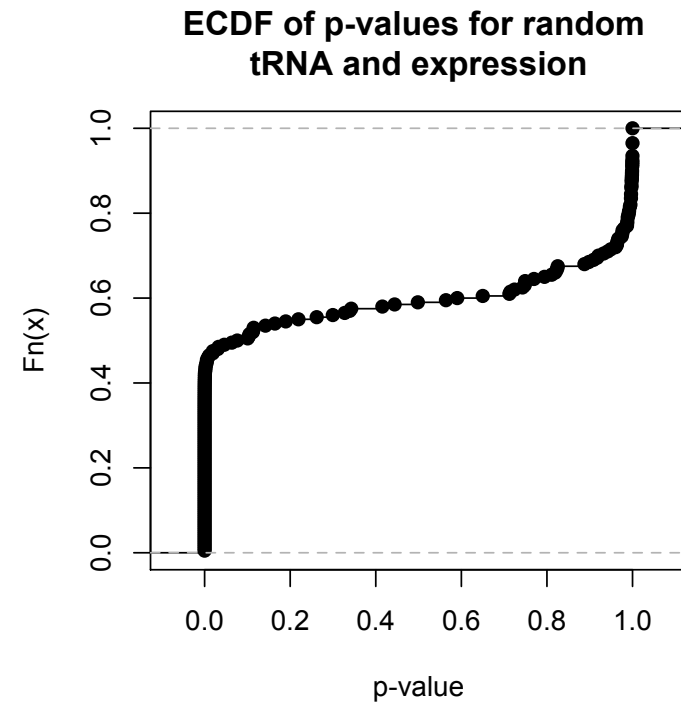
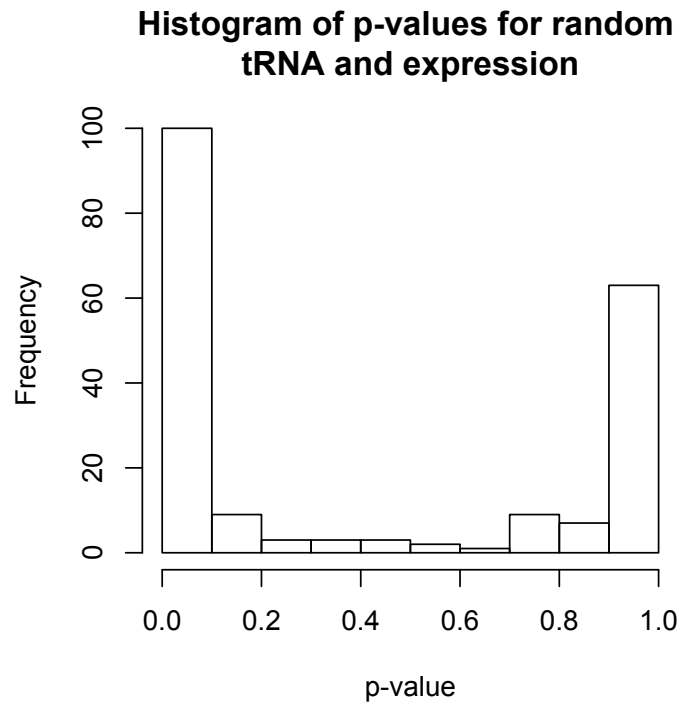
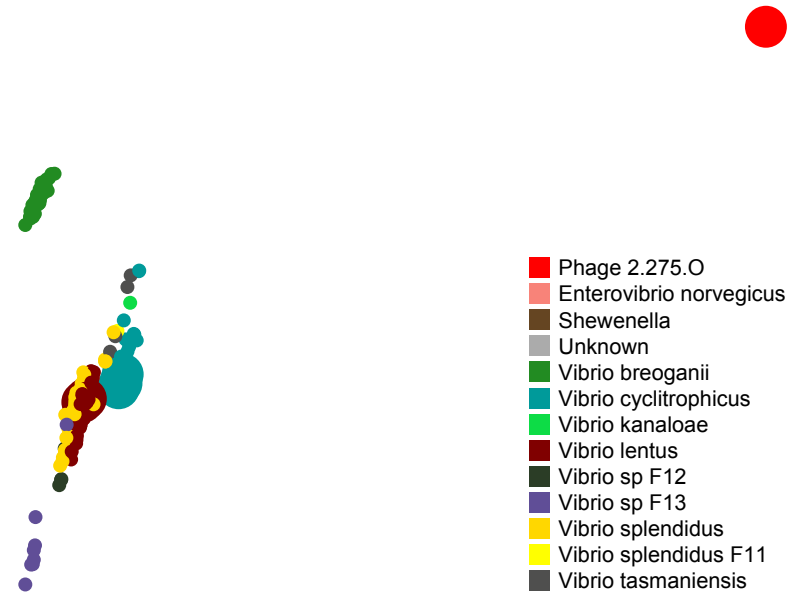


Figure S4. Slant values of phage and host genes, related to STAR Methods. Probability Density Function (left) and Empirical Cumulative Density Function (right) of the p-values for testing whether a significant difference exists between slant values of phage and host genes given simulated random phage tRNA expression vectors. The p-value is usually close to 0 or 1, as we know in advance that: 1. the phage and host genes have different codon usage preferences, and 2. the host tRNA pool is closely matched to the core host genes. So most random phage expression vectors will differentiate the phage slant values from the host slant values. It is then almost a coin flip as to whether the slant of the phage genes is closer to the phage tRNA pool or the host tRNA pool.

MDS of Phage 2.275.O and Vibrios of the Nahant Collection



Shannon Jensen Divergence of Vibrio Codon Usage from Phage 2.275.O

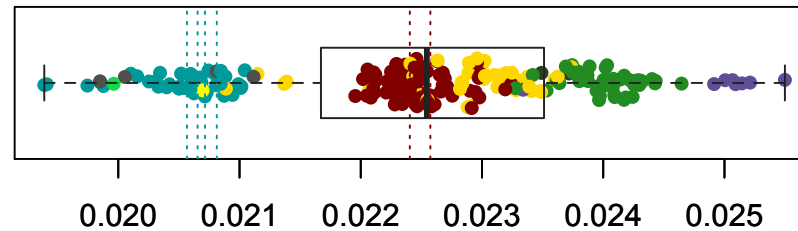


Figure S5. Codon usage for *Vibrio* in the Nahant Collection, related to STAR Methods. The upper panel shows a multidimensional scaling plot of the codon usage Shannon-Jensen divergences in codon usage among various bacteria in the Nahant Collection and phage 2.275.O. Points representing phage 2.275.O and its hosts are highlighted using larger points. As expected, the bacteria in the Nahant Collection cluster by their species. The bottom panel shows the distribution of Shannon-Jensen divergences from phage 2.275.O. Divergence values for hosts of 2.275.O are highlighted by the dotted lines. *V. cyclitrophicus* hosts are more similar in codon usage to 2.275.O than *V. lentus* among which the phage also has hosts.

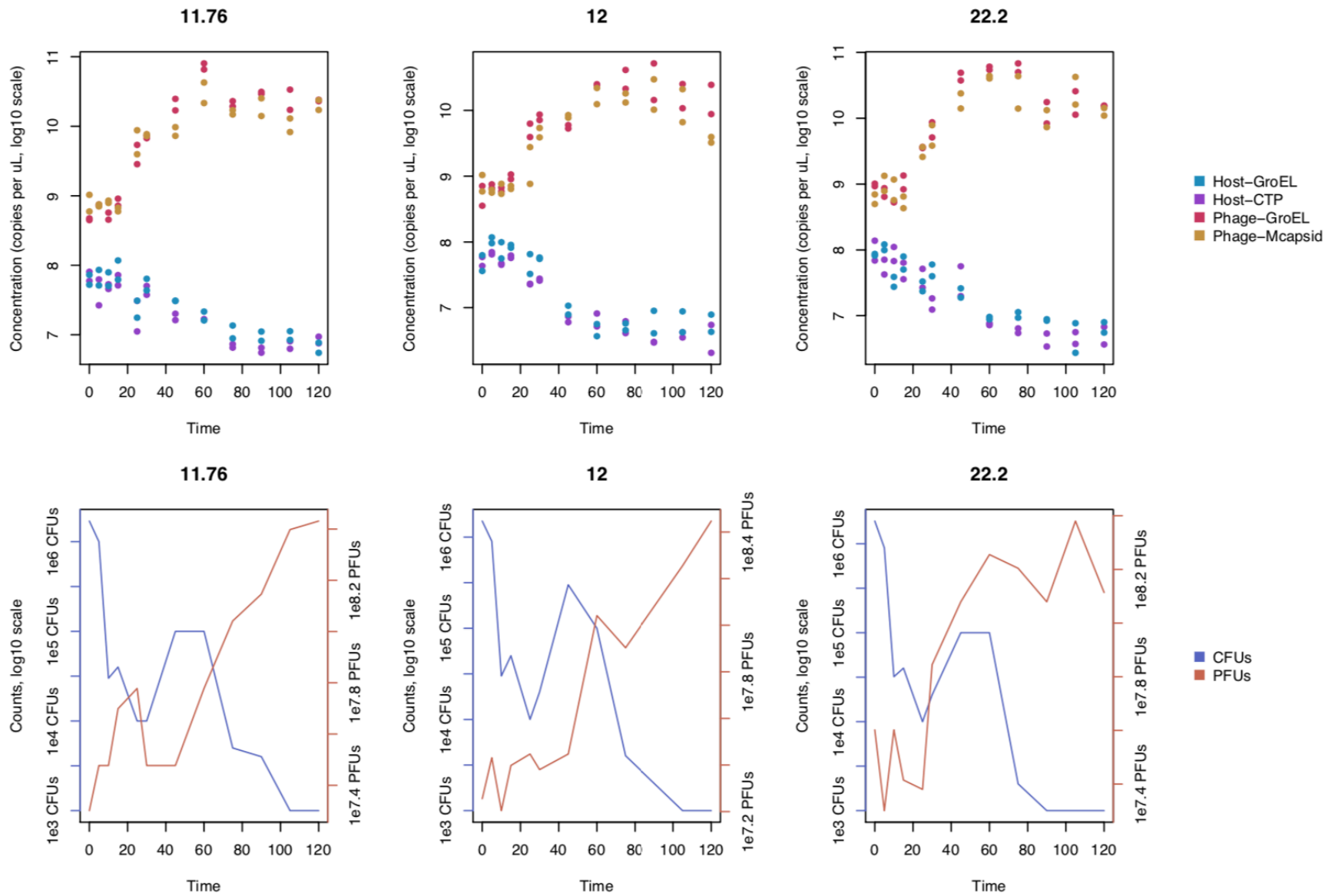


Figure S6, related to Figure 4. Host genome degradation. To demonstrate that the host genome is degraded, we ran another validation experiment. In the graphs above, the first row shows the DNA concentration over time, on log scale, measured by qPCR, and the bottom row shows the number of colony/plaque forming units in 5 uL of culture. Each column of plots is a different trial, labeled with the calculated MOI.

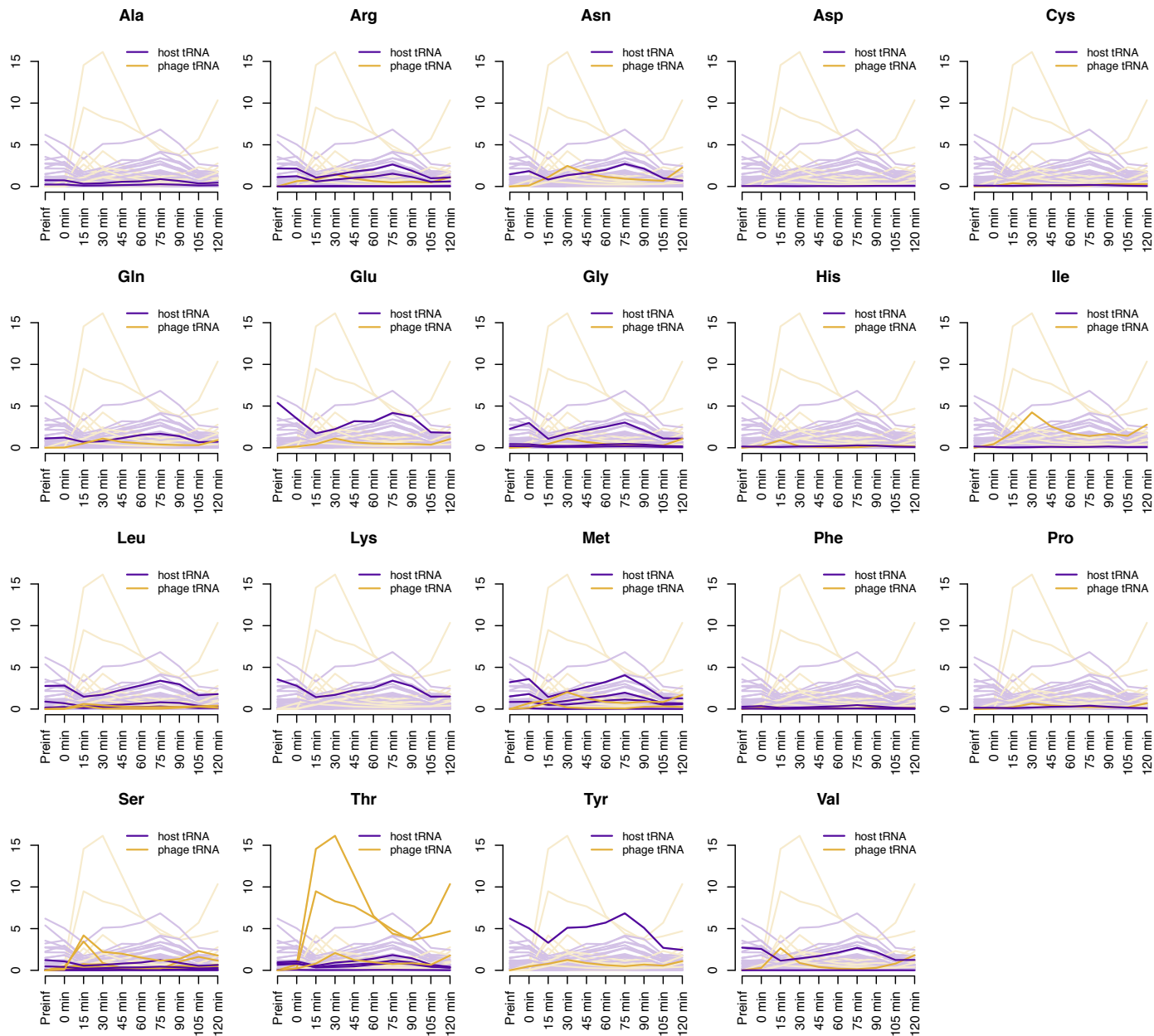


Figure S7, related to Figure 4. The tRNA subset of RNA-seq. Host tRNA are degraded upon infection while phage tRNA rapidly increase. Reads are normalized to a firefly luciferase spike-in for each sample. This supplementary figure expands figure 4C by amino acid.

Correspondence Between Host tRNA Expression and Codon Usage

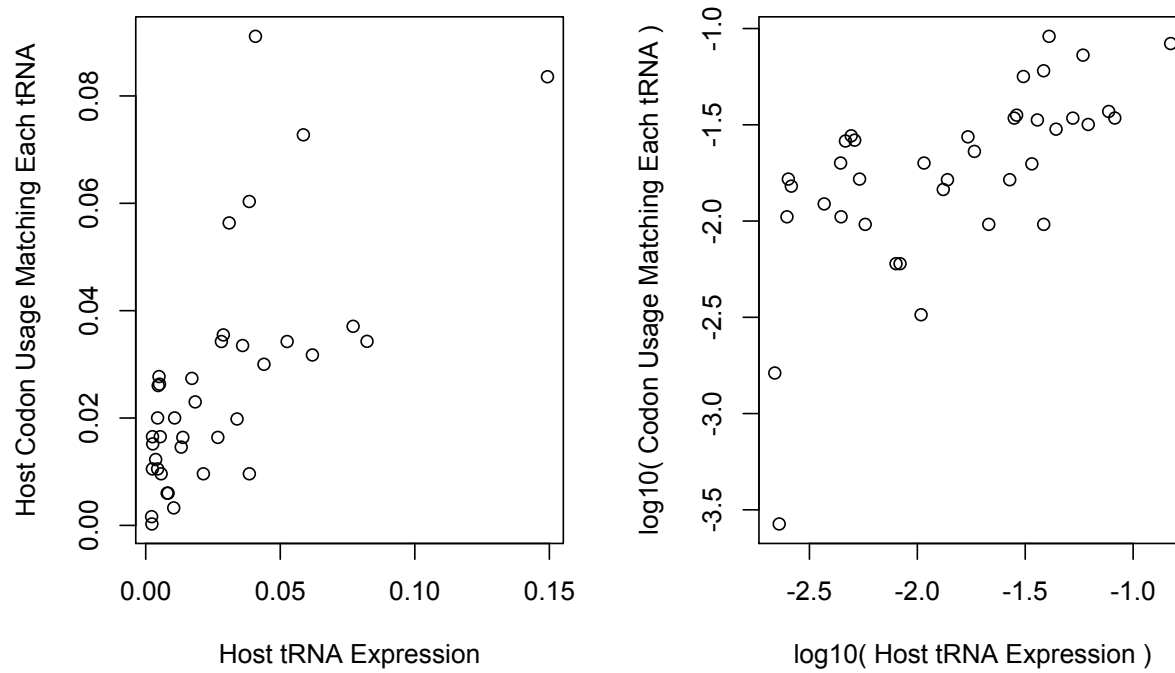


Figure S8. Host tRNA expression and codon usage, related to STAR Methods. Host tRNA expression is correlated with host codon usage. Here, codon usage is weighted by the expression level of each gene pre-infection.

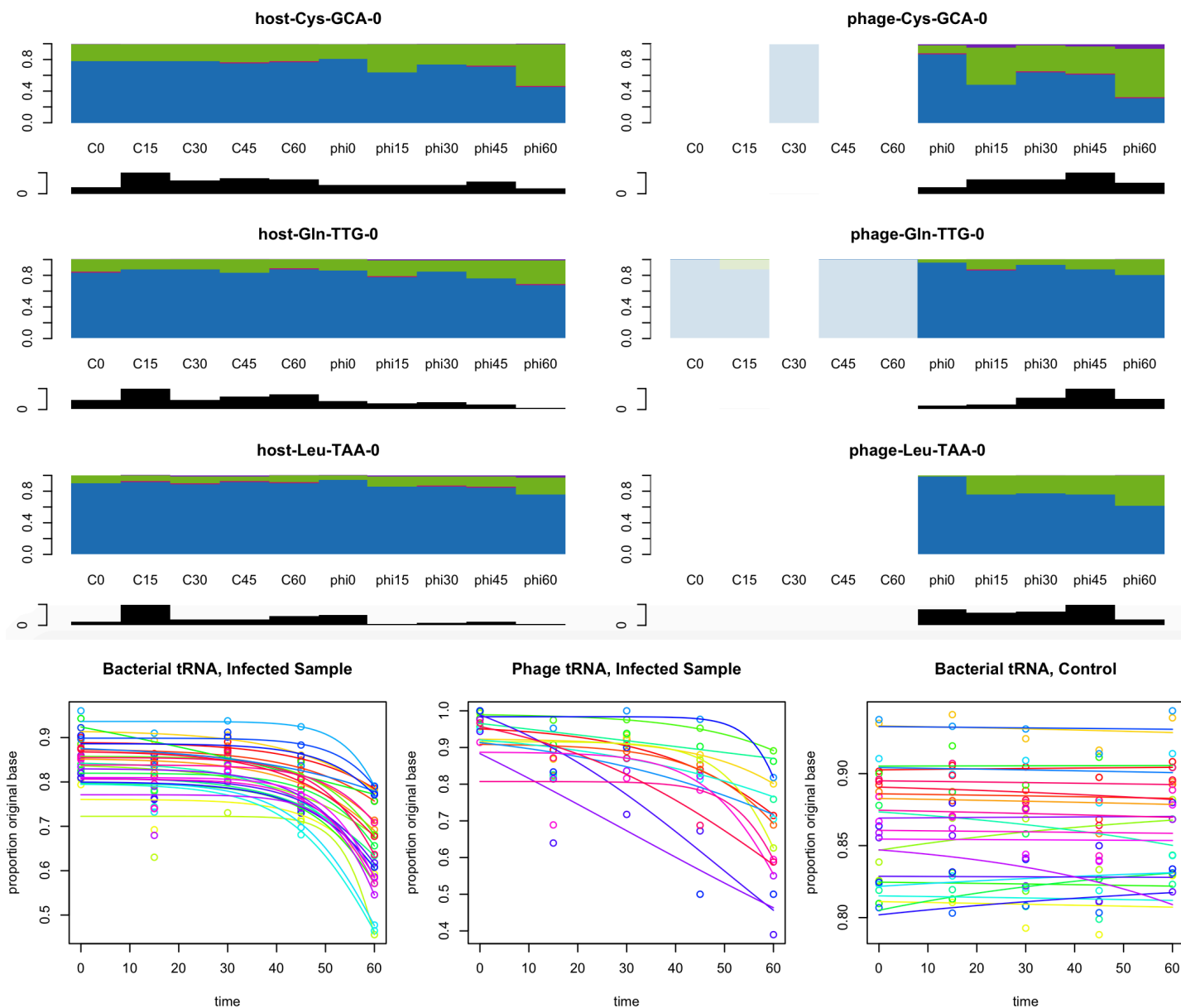


Figure S9. tRNA modification, related to STAR Methods. 4-thiouridine modification of the phage and host tRNA appear to increase throughout the course of infection. Green bars indicate the “missread” C for phage (left panels) and host (right panels) tRNA. This modification may be due to a decrease in nascent tRNA production over time or continued action of modification enzymes.

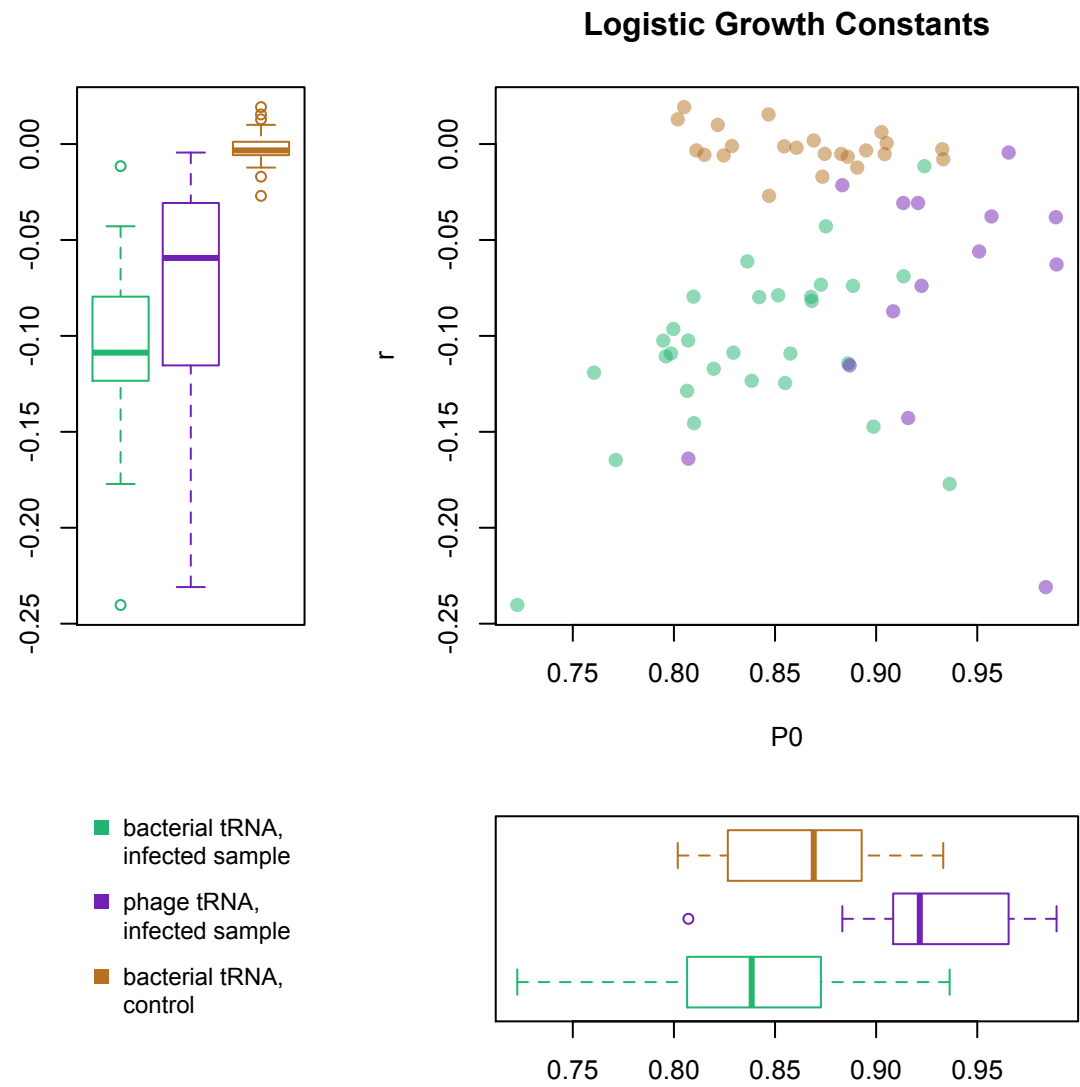
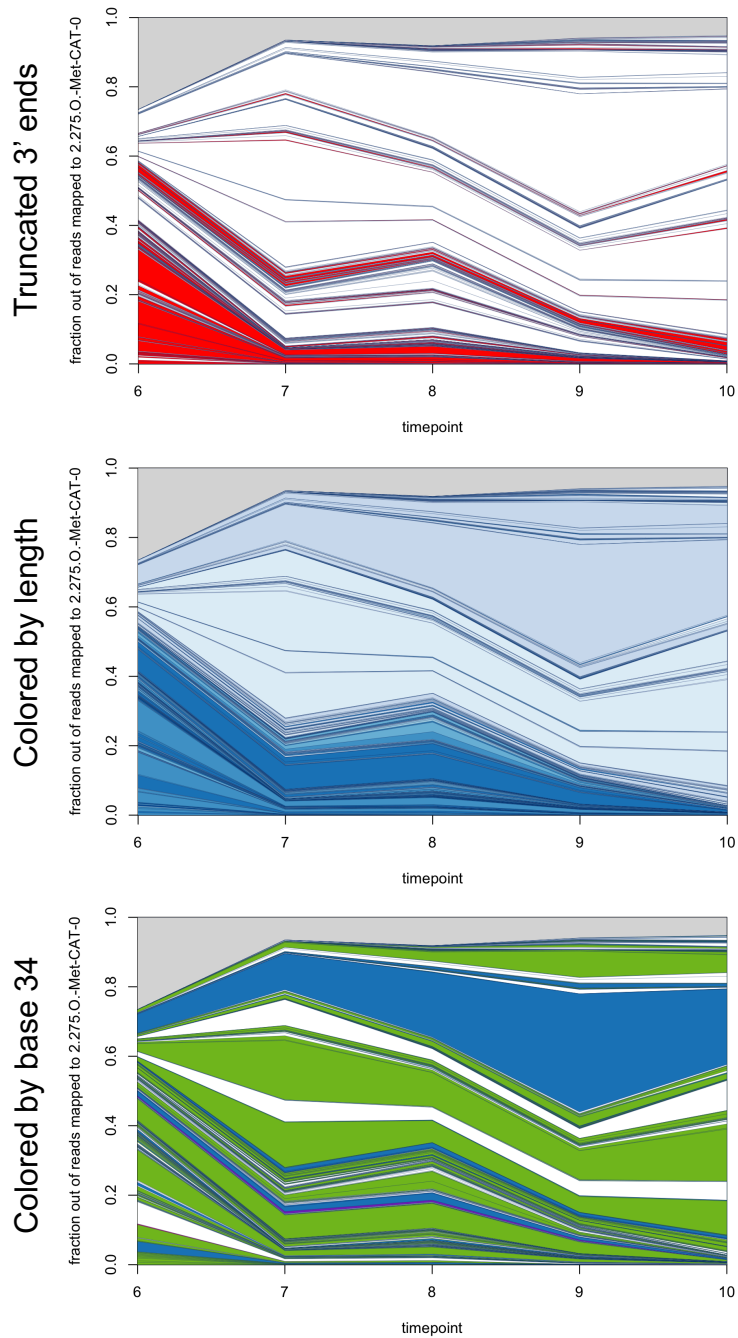


Figure S10. Constants of a logistic growth curve fit to the increase in “missequenced” bases on 4-thiouridine, related to STAR Methods. While phage and host tRNA start off modified at different levels (at the beginning of the timecourse the host tRNA are at equilibrium but the phage tRNA are nascent) the rate of modification is roughly the same for phage and host tRNA, and so both appear to be continually modified, likely through the same process.



Unique species of phage Met-CAT

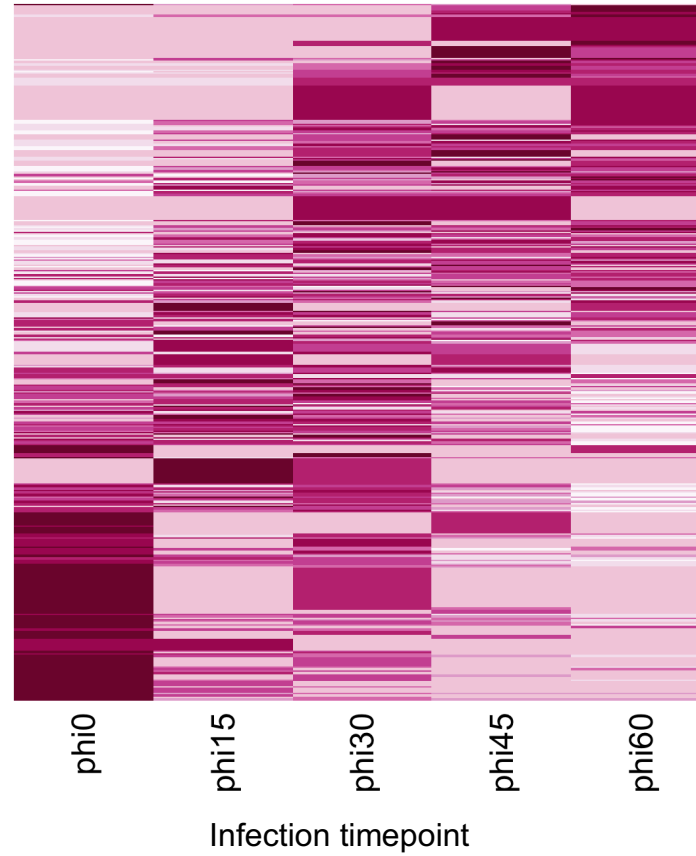


Figure S11. Phage tRNA species change over the course of infection, related to STAR Methods. In the plots to the left, each ribbon represents an Ile-}AT species, and in the plot above, each row represents a phage Ile-}AT species. There appears to be a distinct shift in the predominant species present during different stages of the infection.

tRNA-seq Infection Timecourse

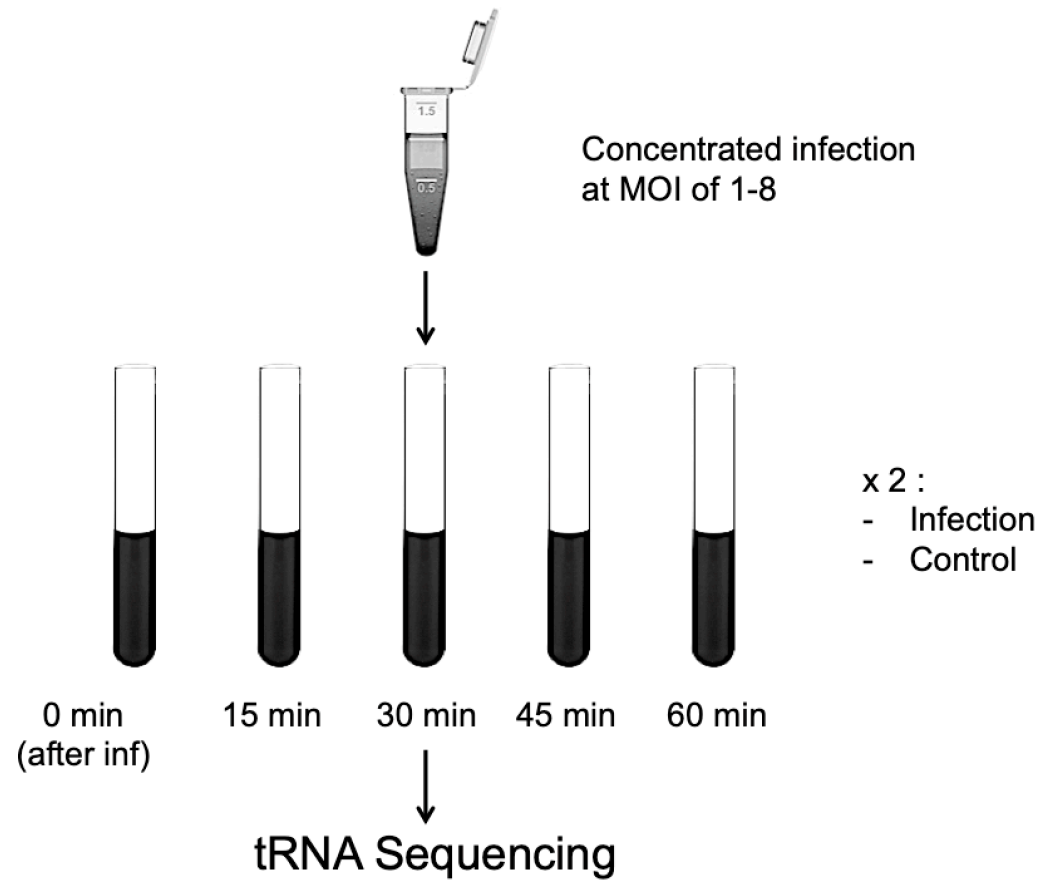


Figure S12. Schematic of tRNA sequencing timecourse, related to STAR Methods.

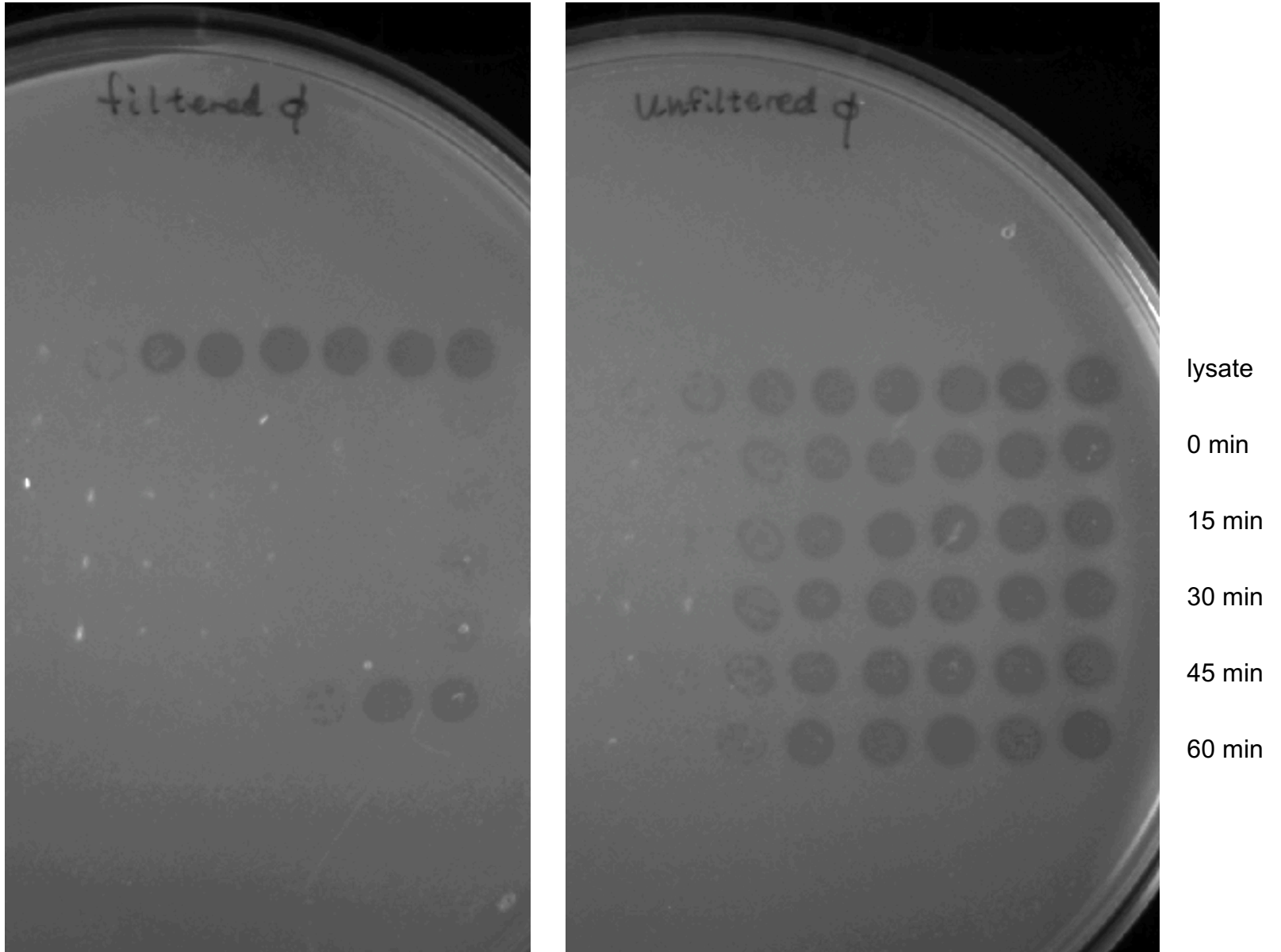


Figure S13. Plaque counts at each stage of the RNA sequencing infection timecourse, related to STAR Methods.

RNA-seq Infection Timecourse

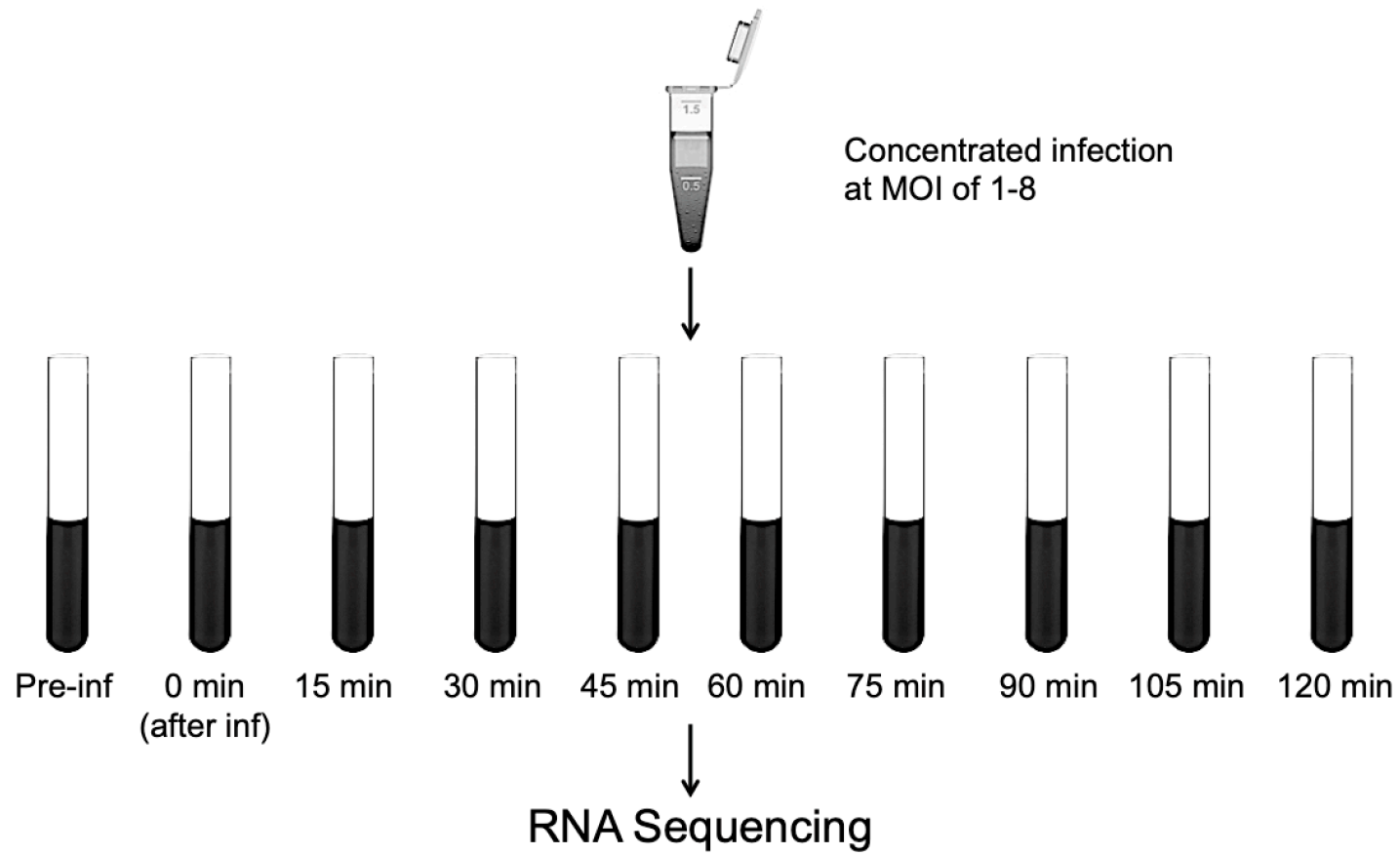


Figure S14. Schematic of RNA sequencing timecourse, related to STAR Methods.

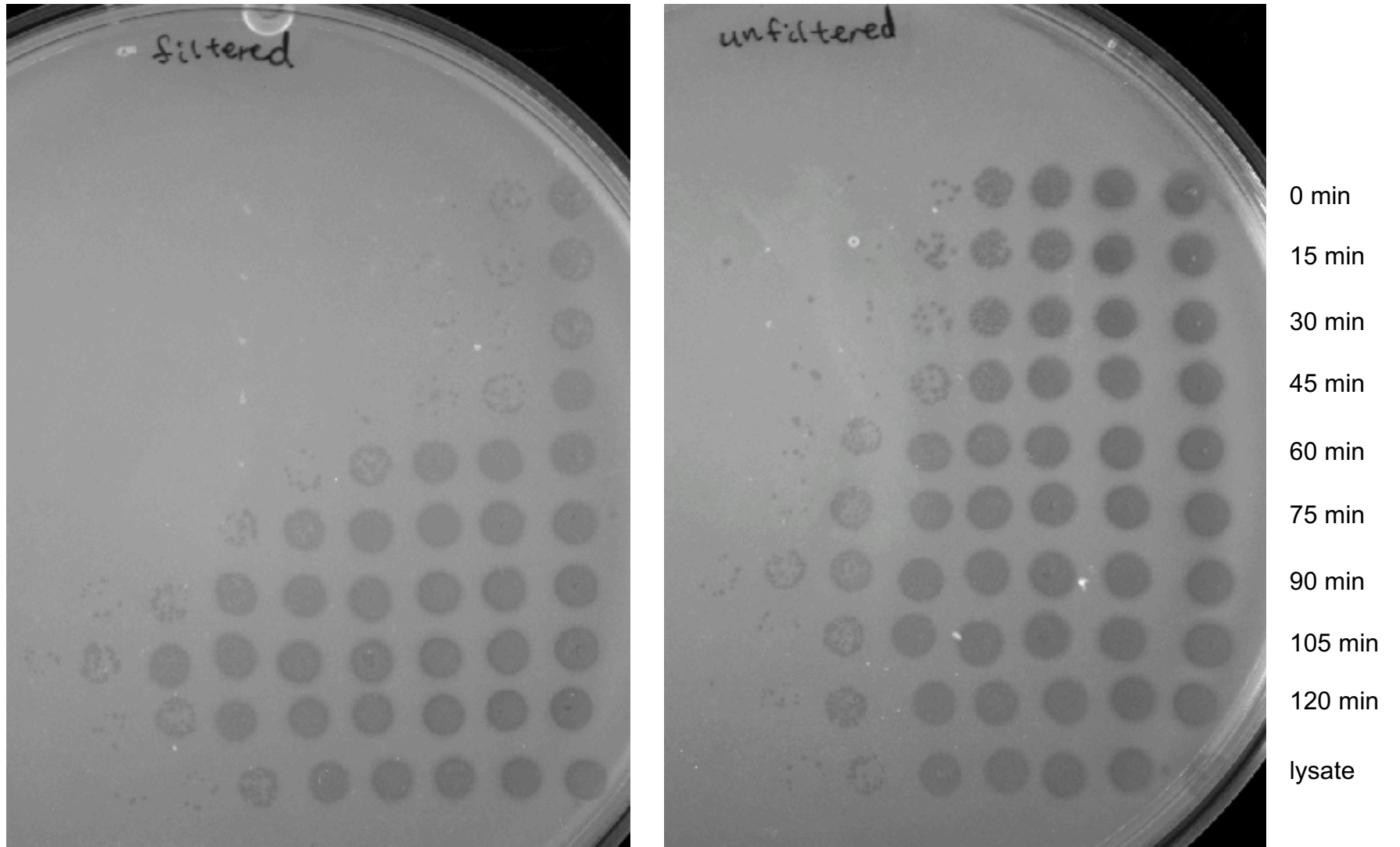


Figure S15. Plaque counts at each stage of the tRNA sequencing infection timecourse, related to STAR Methods.

Log Fold Change Between Time Points

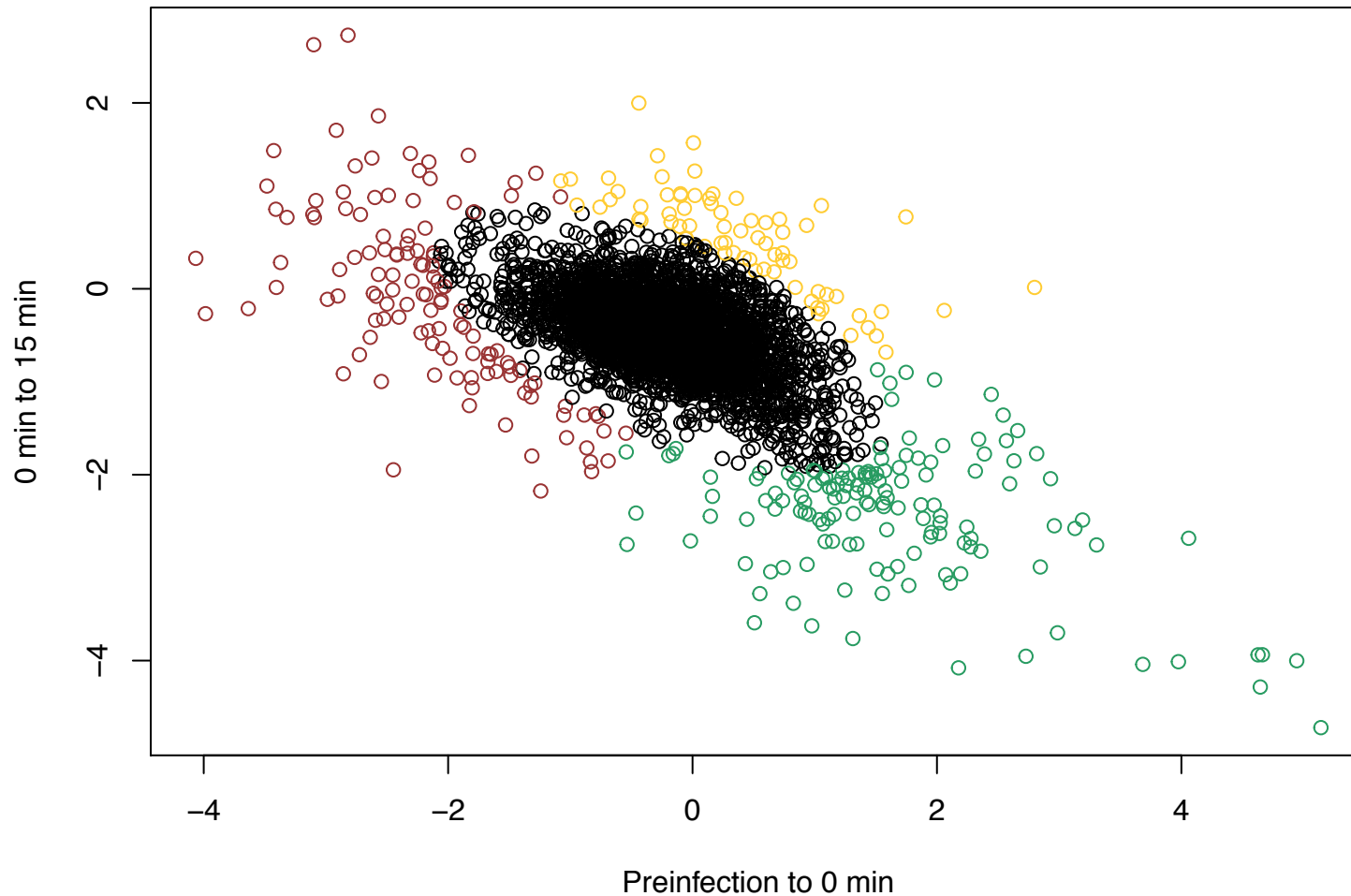


Figure S16. Host gene expression, related to STAR Methods. Host genes were clustered into a “typical” expression pattern and three groups of outliers. Initially, all time points were used for this clustering analysis; however, the patterns found were predominantly determined by the change in expression between the first three time points. Because of this, the focus was narrowed to the first three timepoints. Outliers were determined by examining points whose Mahalanobis distance from the center of the distribution was beyond the 95th percentile of a chi-squared distribution with 2 degrees of freedom. The outliers were then clustered into three groups, shown in Figure S17. A full list of genes in the three outlier groups are included in Table S3.

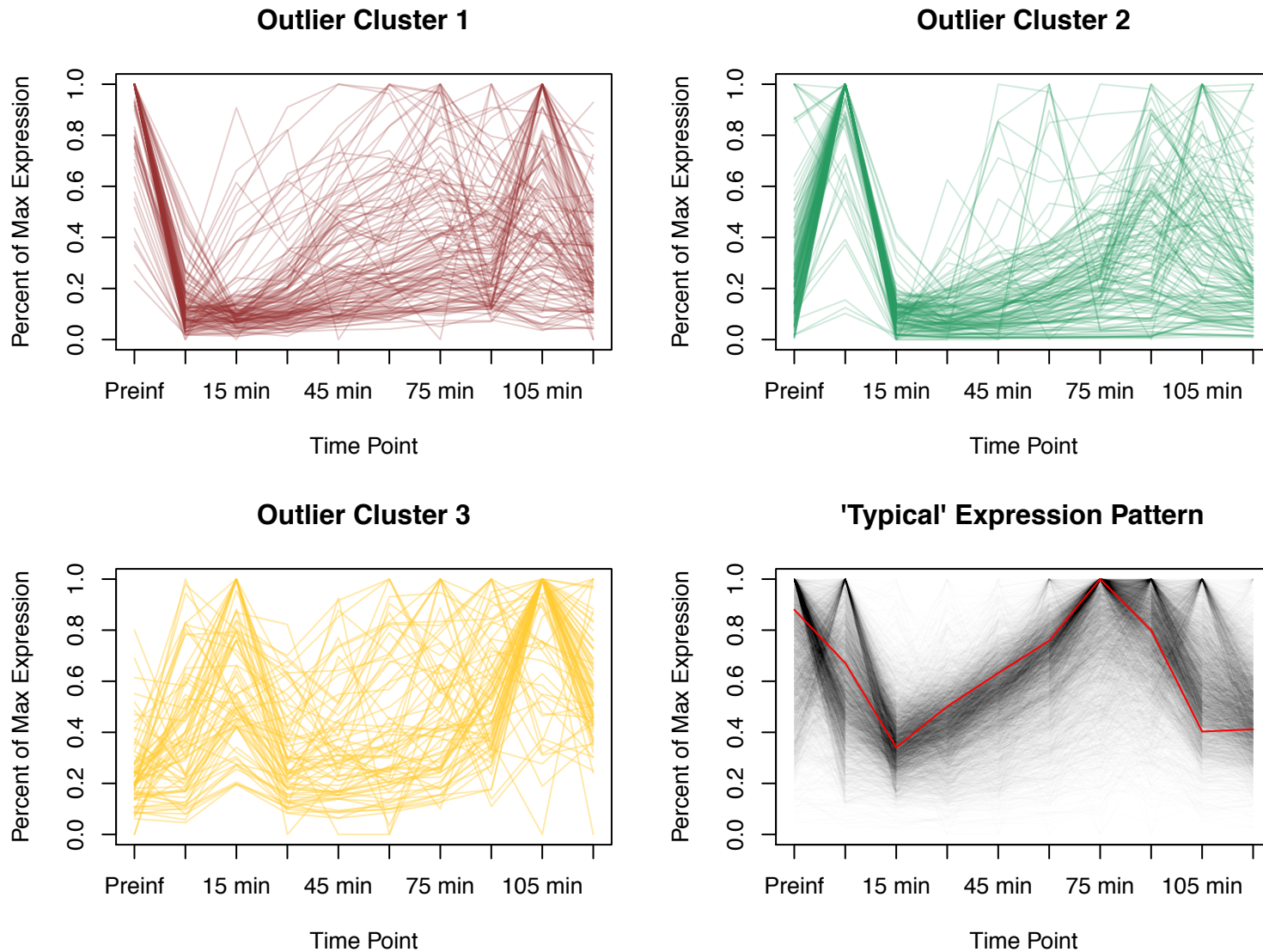


Figure S17. Host gene expression clusters, related to STAR Methods. The first outlier cluster contains genes that immediately decline in expression upon infection. The second outlier cluster contains genes that are expressed/overexpressed upon infection and then are degraded. The third outlier cluster contains genes that slowly increase in expression for the first 15 minutes of infection and then are degraded. And finally, the “typical” expression is defined by degradation (and perhaps some amount of ambiguous fluctuation) leading to an observable trough at around 15 minutes. Ribonuclease P, which is required for 5’ processing of tRNA, follows the “typical” expression pattern. Outlier cluster genes can be found in table S3.

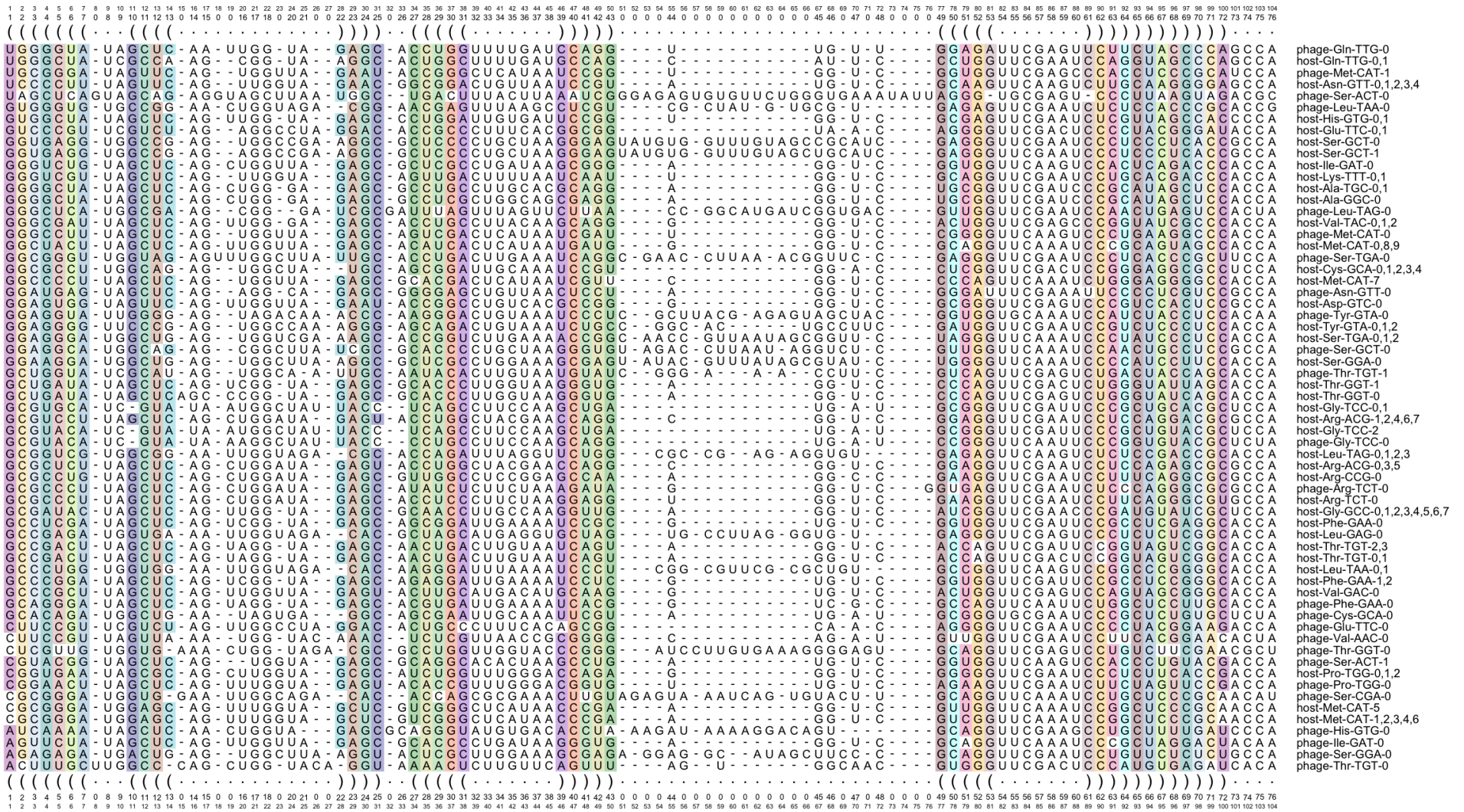


Figure S18. LocaRNA alignment of phage and host unique tRNA sequences, related to STAR Methods. Base paired stem regions are highlighted with the same color, the three-way base pair is highlighted in yellow.

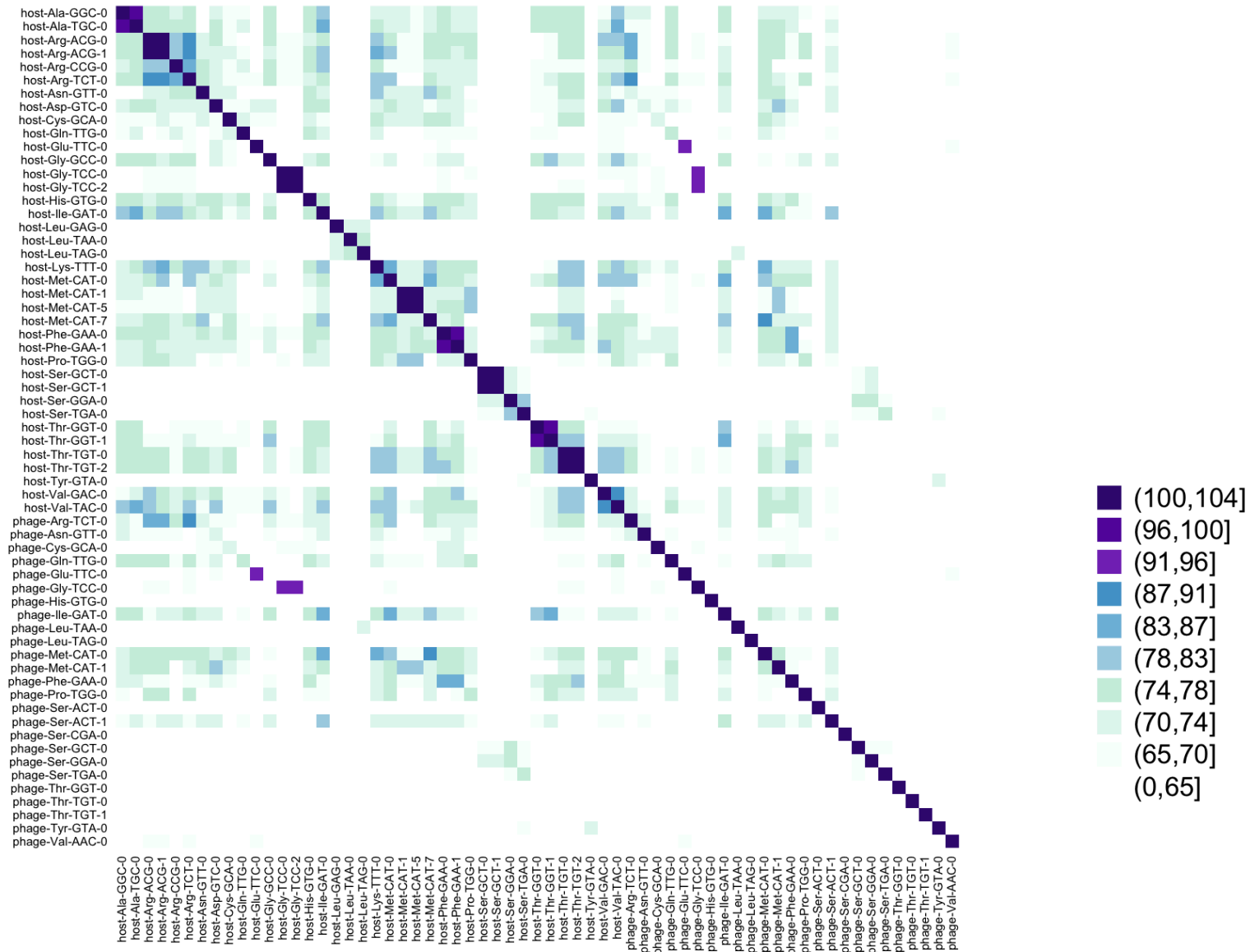


Figure S19. Alignment similarity of phage and host tRNA, related to STAR Methods. Phage tRNA are different enough from host tRNA for reads from tRNA-seq to be mapped back to the correct organism.

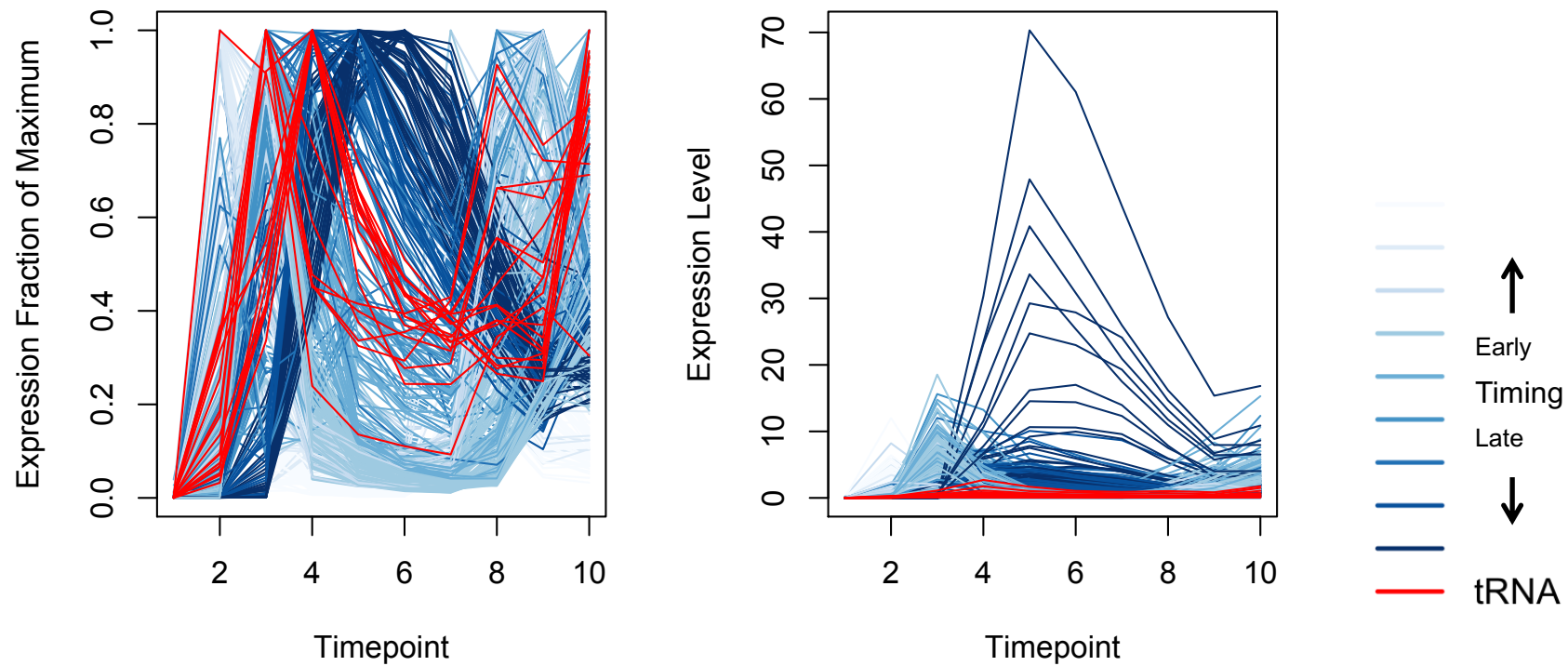


Figure S20. Phage gene expression colored by expression timing, related to STAR Methods and Figure 4. Phage gene expression is color coded according to expression timing as calculated by the center of mass of the first 6 timepoints (the first round of infection). These values are used on the x-axis of Figure 4C and 4D.